Available online at www.sciencedirect.com

SCIENCE DIRECT

Cement and Concrete Research 35 (2005) 213–219

CEMENT AND CONCRETE RESEARCH

Calculating liquid transport into high-performance concrete during wet freeze/thaw

Stefan Jacobsen*

Narvik University College, Lodve Langes gt. 2, 8505 Narvik, Norway

Received 14 December 2000; accepted 29 April 2004

Abstract

A method for calculation of the liquid transport into high-performance concrete (HPC) during wet freeze/thaw exposure is proposed. This transport, or pumping effect, which is larger than absorption above 0 °C, is in the present calculation assumed to be caused by diffusion of water from the wet surface, through hardened cement paste (HCP) where water in nonfreezable, to large voids with very low vapour content. Saturated flow is assumed between the wet concrete surface and the active voids. Cranks solution for stationary transport into a hollow sphere of mean radius $\bar{r}$ is combined with Powers spacing factor. The shell thickness is the mean void spacing factor ($\bar{L}$). The flow into voids was calculated ("good" vs. "bad" void system) for various maximum possible moisture potentials between wet surface, saturated HCP and active void (at 263 K and 1 atm; Δp = saturation pressure = 260 Pa or Δv = moisture content = 0.00215 kg/m^3 in void, etc.). Realistic voids and diffusivity were used. The calculation fits with liquid uptake measured in wet freeze/thaw of HPC with exposed surface equal to the surface of the active voids. The lower the void content, the lower is the pumping effect. Nonstationary transport, further experiments and simulations are discussed briefly.

Keywords: Humidity; Freezing and thawing; Diffusion; High-performance concrete

1. Introduction and significance

The deterioration of concrete by frost, reinforcement corrosion and chemical attack (leaching, sulphate attack, alkali aggregate reactions, etc.) depends mainly on transport properties. Transported matter can be various liquids, gases, dissolved and more or less aggressive ions, concrete constituents, etc. Air entraining is the traditional technology to protect concrete against frost deterioration. High-performance concrete (HPC) with low water/binder ratio (w/b), however, can be very durable without air entraining, even after very severe freeze/thaw exposure in the presence of deicing salt, as found by many researchers [1]. One key factor is that water in the hardened cement paste (HCP) of saturated HPC cannot freeze at winter temperatures [2,3]. Air entraining complicates production, makes HPC more dependent of quality assurance, resulting in a more expensive product. This paper presents a model for prediction of the moisture flow into HPC during wet freeze/thaw, to proceed in the development of frost resistant HPC without air entraining.

2. Discussion of previous research

The most common way of laboratory testing is to expose the concrete to repeated freezing and thawing with liquid on the surface at all times. This wet freeze/thaw exposure leads to a pumping effect [4] with much higher absorption rate compared to the slow long-term absorption rate under isothermal conditions (see Fig. 1). Because the degree of saturation of the concrete will increase dramatically, damage may arise much faster in wet frost testing in the laboratory than in most real exposure situations. The pumping effect was even observed in wet freeze/thaw testing on HPC down to −20 °C where no freezable water was detected in the low-temperature calorimeter on saturated specimens taken from the same concrete binder [3,4]. In Refs. [5,6], the magnitude of the transport caused by the pumping effect and the mechanisms causing this transport were reviewed. For

* Tel.: +47-76-96-60-00; fax: +47-76-96-68-18.
E-mail address: sja@hin.no (S. Jacobsen).

0008-8846/$ – see front matter © 2004 Elsevier Ltd. All rights reserved.
doi:10.1016/j.cemconres.2004.04.029

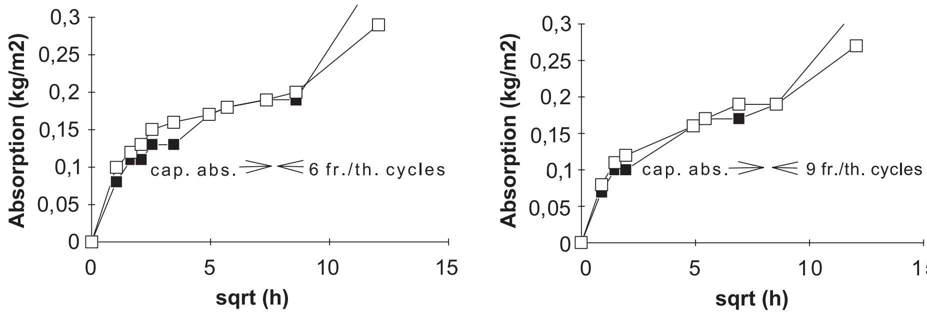

Fig. 1. Pumping effect in 040-05/040-05A (air) concrete, 2.8 and 4.9 °C/h cooling rate [4].

low w/b concrete, it was concluded that the type of mechanism described by Powers and Helmuth [7] is most relevant.

Diffusion of vapour from HCP saturated with nonfreezable water towards large voids with lower vapour pressure will cause more liquid to be absorbed at the wet concrete surface. The driving potentials and associated flow have been quantified for ordinary concrete. Pickett [8] calculated the flow between gel and capillary pores based on Ref. [7] and on diffusion theory. Litvan [9] explained internal flow of water towards large voids somewhat similarly to Powers and Helmuth. Setzer [10] derived the pressure associated with microice lens formation in the cement paste. These authors, however, focused on the deterioration and based their experiments on ordinary Portland cement binders of w/b = 0.4–0.8. Therefore, in their specimens of OPC binders, significant amounts of pore water would freeze down to − 20 °C contrary to HPC where the freezing point depression is much larger.

In an HPC in which water in the saturated HCP cannot freeze down to − 20 °C, but with, say, 2% of voids with as much as 10% of the void volume filled, less than 0.001 g ice/g dry concrete can form as bulk water freezes at 0 °C. This is in the low range of what is reported from low-temperature calorimetry [2–4], but may still cause the kind of vapour diffusion described by Powers and Helmuth [7]. Furthermore, in a concrete with 35 vol.% of paste, ice formation of this magnitude in saturated pores is also lower than the 0.7% freezable water required to create harmful pressure of hydraulic or closed container type at freezing to − 20 °C as calculated by Fagerlund [11]. Therefore, neither external nor internal hydraulic pressure and/or suction seem to be created as driving forces at such low content of freezable water. However, even empty voids cause transport during freezing because their low vapour content creates a potential from the wet surface. Diffusion from the wet surface towards larger pores/voids with low or no water content was therefore proposed as mechanism for the observed liquid uptake [5]. Most probably, the voids are empty at first, but a little bit of condensation of moisture from the air in the pores may freeze as temperature drops.

An estimate of the vapour pressure gradient in saturated HCP adjacent to a void in Ref. [5] was based on transport measured during wet freeze/thaw and assuming steady state flow. Assuming linear vapour pressure gradient and saturated flow, Ficks' first law applies (Eq. (1)):

$$\frac{\mathrm{d}p}{\mathrm{d}x} = \frac{g}{\delta_p} \tag{1}$$

Here, dp (Pa) is vapour pressure difference between saturated HCP and void in which there can be dry air or perhaps ice; dx (m) is length from saturated paste to void where the vapour pressure is at minimum; δ_p (kg/(mPas)) is vapour diffusivity or permeability and g (kg/(m^2 s)) is transport rate. Fig. 2 illustrates this case.

Table 1 shows length of the linear vapour pressure gradient calculated using Eq. (1) for various temperatures.

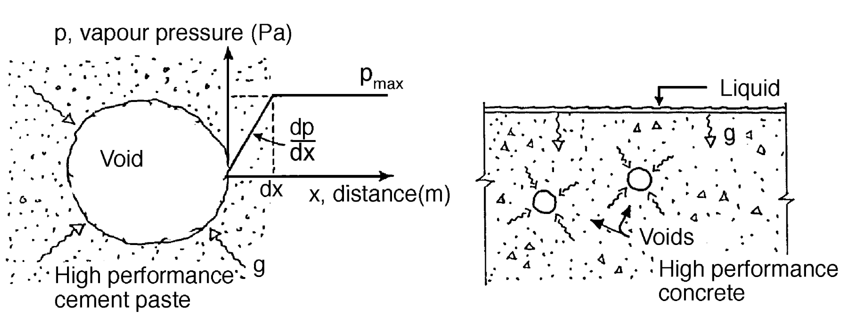

Fig. 2. Vapour flow from saturated HCP towards void [5].

Table 1
Calculated length of the vapour pressure gradient, dx, in Fig. 2.

dp/dx (Pa/m)	dp_{max} (Pa)	Saturation pressure at (°C)	dx in HCP (mm)
2×10^{-6}	550	−1	0.69
	260	−10	0.33
	100	−20	0.13

The maximum possible vapour pressure difference dp, is then equal to the saturation pressure of vapour at the actual temperature and 1 atmosphere. The transport was measured during wet freeze/thaw exposure of high-strength lightweight aggregate concrete in the laboratory [4,5]. It is seen that dx is similar to the critical spacing factor, L_{crit}, needed to protect concrete against wet freeze/thaw.

However, the flow rate towards a spherical void increases when the distance to the void is reduced. The gradient dp/dx of Fig. 2 is therefore not linear [12]. To calculate the flow more accurately, this and some other factors are investigated further in this paper.

3. Diffusion through a thick-walled sphere

In this paper, the HPC is assumed to have saturated HCP in which water vapour can flow but not freeze. This assumption is based on the two experimental observations already described: (1) liquid uptake in HPC is increased during wet freeze/thaw compared to at isothermal absorption (the pumping effect) and (2) water cannot freeze in the same concrete in the temperature range of the frost test. One can imagine this material as one with only gel-type pores that are saturated.

As a first attempt towards more realistic calculation of the transport into HPC during wet freeze/thaw exposure, the diffusion is calculated as going into a thick-walled sphere. The global transport is still assumed stationary. The latter is most realistic for the saturated HCP closest to the surface of a continuously wet HPC. This is done according to Crank [13] (see Fig. 3 and Eq. (2)).

$$G = 4\pi\delta_p \frac{ab}{b-a}\Delta p \tag{2}$$

G (kg/s) is flow rate into the void, and Δp (Pa) is the vapour pressure difference over the shell wall of thickness $(b-a)(m)$. Powers spacing factor, $\bar{L}$, is based on hydraulic flow [14] but expresses the air void distribution as a mean concrete thickness smeared over the surface of the air voids. Using the parameters of Cranks solution, we then have:

$$b - a = \bar{L} \tag{3}$$

$$a = \bar{r} \tag{4}$$

$$b = \bar{L} + \bar{r} \tag{5}$$

with the mean spacing factor $\bar{L}$ (m) and mean void radius $\bar{r}$ (m). The simplification Eqs. (3)–(5) does not give a 100% realistic air void system, but an estimate of the shell thickness in a stationary diffusion calculation. Snyder [15] has analysed various studies and equations for void spacing, including overlapping of shells, 3D and effect of size distribution of the voids, as a basis for further improvement. Snyder et al [16] also studied hydraulic flow into voids in HPC during wet freeze/thaw and found that HPC could be very freeze/thaw resistant when properly cured. However, real flow was not measured in their tests.

The transport in Eq. (2) given as flow into a void of radius $\bar{r}$ is then

$$G = g4\pi\overline{r^2} \tag{6}$$

if the surface area of the active voids is equal to the exposed concrete surface area. [If the area of the active voids, $A_{active\ voids}$, is larger than the exposed concrete surface area, $A_{exp\ surface}$, the relation between flow through exposed concrete surface, $g_{exp.surface}$, and flow through active void surfaces, $g_{active\ voids}$, is: $g_{exp\ surface}=(A_{active\ voids}/A_{exp\ surface})g_{active\ voids}$]. By combining Eq. (2) with Eqs. (3)–(6), the relation between stationary diffusion and void spacing in HPC can be expressed as:

$$g\overline{r^2} = \delta_p \Delta p \left(\bar{r} + \frac{\overline{r^2}}{\bar{L}}\right) \tag{7}$$

The diffusivity, δ_p, is assumed constant in the saturated HCP. Eq. (7) can also be expressed as

$$\bar{L} = \frac{\bar{r}}{\frac{g\bar{r}}{\delta_p \Delta p} - 1} \quad \text{where}$$

$$\frac{g\bar{r}}{\delta_p \Delta p} = F(\text{Frost factor}) > 1 \text{ is dimensionless} \tag{8}$$

If $F \leq 1$, the expression (8) has no meaning. We then have a void- (and microdefect-) free system without driving

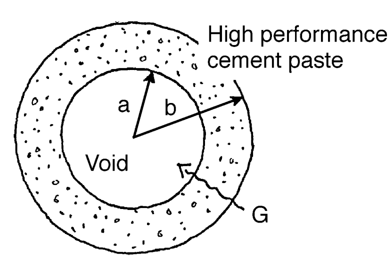

Fig. 3. Diffusion into an air void with a shell of cement paste [13].

forces for transport into the material when $\bar{L} \rightarrow \infty$. Compared to traditional experiences with the protective effect of air voids, the following F values yield:

$$F = 2 \Rightarrow \text{fair air void system}(\bar{L} = \bar{r})$$

$$F = 1.1 \Rightarrow \text{bad air void system}(\bar{L} = 10\bar{r})$$

Stationary transport into an air void during wet freeze/thaw exposure, the pumping effect illustrated in Fig. 1, is then:

$$g = \left[\frac{F}{F-1}\right]\delta_p \frac{\Delta p}{\bar{L}} \tag{9}$$

4. Results and discussion

4.1. Flow into void

Table 2 shows the rate of stationary transport into a void according to Eq. (9). Various temperatures and thus maximum possible vapour pressure differences from wet surface, through saturated paste and into the void, have been used. δ_p was set at 10^{-13} kg/(mPas). This is a very low value [17], realistic near the wet surface where the HCP can be assumed saturated. Fig. 4 shows flow as function of void characteristics for $\Delta p = 260$ Pa and $\delta_p = 10^{-13}$ kg/(mPas). We see that for the particular data, a large variation in void characteristics causes flow to vary almost two decades.

The moisture transport into HPC with lightweight aggregate (LWA) was measured during wet freeze/thaw [4,5]. The flow, g, was found to be in the order of $4.7–9.3 \times 10^{-7}$ kg/m^2 s in the period with frozen material and wet surface. Flow of similar magnitude was also observed in several other HPCs in Ref. [4] during wet freeze/thaw, e.g., the absorption after start of freeze/thaw in Fig. 1. In addition, many other researchers observed flow in this order, as found in the review [5]. There are some uncertainties about the real vapour pressure difference between the wet surface and the void, as well as amount of active voids. Still, Table 2 indicates that the proposed approach can be used in the further modelling of this transfer problem.

The w/b of the above LWA concrete was 0.35 with 8% silica fume. The content of freezable water in the HCP was

Table 2
Steady state transport into a void at the surface of saturated HPC, Eq. (9)

Temperature (°C)	Δp_{max} (Pa)	Maximum moisture transport, g (10^{-7} kg/m^2 s)	
		Good air void system, $\bar{L}$=0.33 mm, F=2	Bad air void system, $\bar{L}$=3.3 mm, F=1.1
−1	550	3.3	1.8
−10	260	1.6	0.9
−20	100	0.6	0.3

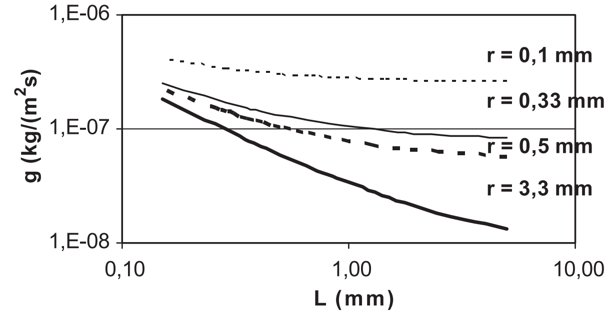

Fig. 4. Effect on flow of various void systems for $\Delta p = 260$ Pa and $\delta_p = 10^{-13}$ kg/(mPas).

measured to be zero in a low-temperature calorimeter down to −20°C [4]. The concrete had no frost damage (scaling, cracking), neither in 300 rapid freeze/thaw cycles in water nor in 98 freeze/thaw cycles with deicer salt. It is therefore realistic to assume zero ice formation in the HCP throughout the actual freeze/thaw exposure period. If there is freezable water in the HCP, due to high w/b or pore structure coarsening, microice lenses can form and cause destructive pressure according to Ref. [10].

The progression of deterioration in this case was studied in Ref. [4]. Bager and Jacobsen [18,19] described the process thoroughly based on a series of Nordic cooperative research projects.

4.2. Depth of saturation, x_{sat}

The concept depth of saturation was discussed by Powers [20] for hydraulic pressure. In the following, a rough attempt to estimate this figure is performed based on the present idea of transport. Let the surface area of the active voids be equal to the exposed surface of the concrete specimen [$A_{\text{exp surface}}$ (m^2)]. The surface area of the total void content in the concrete specimen is A_{voids} (m^2). Furthermore, the HCP near the wet surface, around the active voids, is assumed saturated. Then, f_{sat} (m^3/m^3), the volume fraction of surface concrete with active voids and saturated HCP, is:

$$f_{sat} \approx \frac{A_{\text{exp surface}}}{A_{\text{voids}}} \tag{10}$$

The depth of saturation, x_{sat} (m), is under these assumptions:

$$x_{sat} \approx \frac{V_{\text{spec}} f_{sat}}{A_{\text{exp surface}}} \approx \frac{V_{\text{spec}}}{A_{\text{voids}}} \tag{11}$$

where V_{spec} (m^3) is specimen volume. Table 3 shows the void parameters of the w/b = 0.35 HPC, including voids in the LWA [4,5]. It can be seen that the void spacing was poor compared to traditional spacing requirements of $\bar{L} \approx 0.25$

Table 3
Void spacing characteristics of HPC with LWA exposed to wet freeze/thaw [4]

Property	Parameter	Quantity
Void characteristics (ASTM C457)	Air content	1.7 vol.%
	Spec. surface	8.1 mm^{-1}
	L	1.3 mm
Characteristics of LWA	Content	41.3 vol.% (43.7 vol.% pores)
	Spec. surface	0.75 mm^{-1}
	HCP layer on LWA	1.9 mm

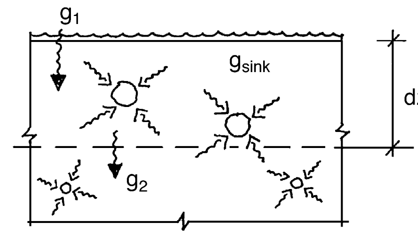

Fig. 5. Nonsteady state flow situation into HPC with voids.

mm for frost protection. The spacing of the highly porous LWA, calculated by smearing the concrete over the LWA surface, was similar to the spacing of air voids.

The depth of saturation can then be estimated for the two test methods and the concrete investigated in Ref. [3] using Eq. (11) (see Table 4). The low depth of saturation estimated in Table 4 is in accordance with measurements of moisture profiles in HPC. Nilsson [21] observed that the humidity of HPC dropped rapidly from surface and inwards even after long-time water storage. The concrete in Ref. [21] had not been freeze/thaw exposed. Furthermore, the present estimate is very coarse. However, this indicates that at the start of freeze/thaw exposure, transport can be very high at the surface.

4.3. Nonstationary flow and sink-term, g_{sink}

The assumption of steady state will make the calculated flow too high, more so the larger portion of the specimen that is counted in when using Eq. (9). The nonstationary transport into a unit area of concrete surface can be calculated by assuming a unidirectional vapour pressure gradient. The flow into each void, as given by Eq. (9), must then be superimposed as a "sink term", g_{sink}. Fig. 5 illustrates this case.

If using vapour content, v, instead of vapour pressure, p, as driving potential, the vapour diffusivity or permeability δ_v (m^2/s) must be used. Then, $\Delta v = 0.00215$ kg/m^3 of pore air instead of $\Delta p = 260$ Pa for saturated air at -10 °C and atmospheric pressure, etc. For a nonsteady state flow description, the vapour content, v (kg/m^3), as function of time and length must then be calculated. According to Nilsson [17], the translation of δ_p (kg/mPas) to a description in vapour content, v, is given by:

$$\delta_v = \frac{RT}{m}\delta_p \tag{12}$$

Here, δ_v = vapour diffusivity (m^2/s), R = gas constant = 8.314 (J/K mol), T = absolute temperature (K) and m = molar mass of water (0.018 kg/mol). At $T = 263$ K ($= -10$ °C):

$$\delta_v \approx 1.215 \times 10^6 \delta_p \tag{13}$$

This is of the same magnitude as found experimentally by Hedenblad [22]. However, the transport mechanism (diffusion or permeation) in HPC can complicate the calculation. Most certainly, we only have diffusive transport in HPC. Most experimental data, however, include both types. Ficks' second law yields for vapour concentration gradient driven transport:

$$\frac{dv}{dt} = -\frac{RT}{m}\delta_p \frac{d}{dz}\left(\frac{dv}{dz}\right) = -\delta_v \frac{d}{dz}\left(\frac{dv}{dz}\right) \tag{14}$$

[Here, it is important not to mix vapour diffusivity δ_v (m^2/s) with diffusivity D (m^2/s) based on total water content (kg/m^3 concrete). The water content is obtained via the sorption isotherm.] By superimposing the "sink term," g_{sink}, Eq. (9) on Eq. (14), the following kind of expression is obtained:

$$\frac{dv}{dt} = \delta_v \frac{d}{dz}\left(\frac{dv}{dz} - \frac{F}{F-1}\cdot\frac{dv}{\bar{L}_{\text{act voids}(z)}}\right) \tag{15}$$

$\bar{L}_{\text{act voids}}(z)$ is the spacing of active voids going down to a certain depth. Eq. (15) can be solved for various assumptions on vapour diffusivity, amount of active voids, vapour pressure, period of freezing in wet condition, period of freezing with sealed surface, etc. In such a case, the

Table 4
Estimated depth of saturation, x_{sat}

Parameter (Eqs. (10) and (11))	Test method: SS 137244	ASTM C666
A_{voids} (m^2)	0.503 (0.05 × 0.15 × 0.15) m^3 × (0.413 × 750 + 0.017 × 8100) m^{-1}	1.566 (0.05 × 0.15 × 0.15) m^3 × (0.413 × 750 + 0.017 × 8100) m^{-1}
$A_{\text{exp surface}}$ (m^2)	0.0225	0.16
f_{sat} (m^3/m^3)	0.0225/0.503 = 0.045	0.16/1.566 = 0.102
V_{spec} (m^3)	(0.05 × 0.15 × 0.15) = 0.001125	(0.1 × 0.1 × 0.35) = 0.0035
x_{sat} (mm)	2–2.5	

Surface area of active voids = specimen surface.

transport coefficient would, however, vary strongly as moisture content is reduced and it would perhaps be better to use the flow potential [22].

4.4. Discussion—modelling and experiments

The higher vapour content in the surface concrete [21] (resulting in increased δ_v and more active voids near the surface) supports the simplification that the surface layer is saturated but with steep moisture gradient below (see Table 2). However, there are additional effects. Temperature gradients will cause moisture movement of the kind described by Eq. (14) in all porous materials. For HPC exposed to wet freeze/thaw, the most probable situation is that the surface is sealed by ice during freezing, unless salt is present. This will stop moisture on its way out towards the cold surface. (A propagating ice front can force water inwards as described by Powers [20] if there is significant ice formation in the pore system of a material, or if there is an external confinement by ice pressure [5].) During thawing, on the other hand, it is more probable that there is ice and/or that the vapour pressure is low inside the concrete while the surface is wet and warmer, sucking or driving moisture into the concrete. Clearly, both heat and mass transfer are important. Such considerations should be included in numerical simulations. In addition, the discussion by Setzer [10] indicates that multiphysics models can be used. Relevant experimental setups and other possible modelling approaches are for example Refs. [4,23–29].

Some important parameters to be measured during wet freeze/thaw in the further study are:

- moisture transport/uptake
- ice formation/freezable water
- length change of material during freeze/thaw
- void characteristics, including spacing of microdefects near the surface
- depth of saturation
- vapour permeability
- measurements of relative humidity (RH) at microlevel
- temperature distribution in concrete and surrounding liquid.

In addition, deterministic service life calculations are possible. The maximum exposure period to wet freeze/thaw before a critical degree of saturation is reached will then be an initiation period [30]. The actual exposure situation is then a frozen concrete with liquid available at an ice-free surface. Using the flow of Table 2, it can be found that the service life of the particular HPC can be very short at the surface of the concrete (days) for this very aggressive exposure situation. Outside the laboratory, however, the access of liquid is often low, which is of course positive for service life. Finally, mechanisms for larger inflow than outflow should be studied as indicated by Jepsen [31], who differentiated between reversible and irreversible water uptake. Some reasons for this irreversibility are now investigated by the present author (exposed surface vs. void surface, self desiccation, free energy of adsorbed water, suction created by crack opening, etc.).

5. Conclusion

Estimates based on measured flow during wet freeze/thaw indicate that diffusion is the most relevant transport mechanism causing the accelerated moisture uptake, or pumping effect, in wet freeze/thaw exposure of HPC. The transport is assumed to be diffusion of nonfreezable water from the wet surface via HCP to the voids. Calculations based on the combination of Powers spacing factor and Cranks solution for diffusion in a thick-walled sphere further support that the pumping effect measured in wet freeze/thaw of HPC is caused by diffusion. Improvements on the understanding of the pumping effect can be made combining improved modelling with instrumented wet freeze/thaw exposure. The most important physical parameters to be measured are as follows: moisture transport, length change, void characteristics (including spacing of microdefects near the surface), depth of saturation, ice formation, relative humidity at microlevel, vapour permeability, and temperature distribution in concrete and surrounding liquid.

Acknowledgements

Thanks to project manager Kim Robert Lisø at NBI, Norway for support and Ken Snyder of NIST, USA, for discussions and valuable suggestions.

References

[1] J. Marchand, R. Gagne, M. Pigeon, E. Sellevold, S. Jacobsen, The frost durability of HPC, in: K. Sakai, N. Banthia, O. Gjørv (Eds.), Consec 95, E & FN Spon, London, 1995, pp. 273–288.

[2] T.A. Hammer, E.J. Sellevold, Frost resistance of HSC, 2nd Int symp High Strength C, ACI SP121, Berkeley, USA, 1990, pp. 457–489.

[3] E. Sellevold, S. Jacobsen, Ice formation and frost salt scaling of concrete: effect of curing temperature and condensed silica fume on normal and HSC, in: P.E. Petersson (Ed.), SP Report 1991:32, Borås, Sweden, 1991, pp. 21–23.

[4] S. Jacobsen, Scaling and cracking in unsealed freeze/thaw testing of OPC and CSF concrete, dr.ing thesis 101:95, Norw.Inst. of Techn., Trondheim, 1995, 286 pp.

[5] S. Jacobsen, Liquid uptake mechanisms in wet freeze/thaw: Review and modelling, in: D.J. Janssen, M.J. Setzer, M.B. Snyder (Eds.), RILEM Proceedings PRO 25, Cachan, France, 2002, pp. 41–51.

[6] S. Jacobsen, Environmental and concrete ageing effects on transport, in: R.D. Hooton, M. Thomas, J. Marchand, J.J. Beadoin (Eds.), Materials Science of Concrete: Ion and Mass Transport in Concrete, Am. Cer. Soc., Westerville, OH, 2001, pp. 13–27.

[7] T.C Powers, R.A. Helmuth, Theory of volume changes in HCP, Highw. Res. Board Proc. 32 (1953) 285–292 (Washington, DC).

[8] G. Pickett, Theory of volume changes in HCP, Highw. Res. Board Proc. 32 (1953) 276–284 (Washington, DC).
[9] G.G. Litvan, Frost action in cement paste, Matér. Constr 6 (34) (1973) 293–298.
[10] M. Setzer, Micro-ice-lens formation in porous solid, J. Colloid Interface Sci. 243 (2001) 193–201.
[11] G. Fagerlund, Frost Resistance of High Performance Concrete: Some Theoretical Considerations, Report TVBM 3056, Lund Inst. Of Tech., Sweden, 1993, 38 pp.
[12] K. Snyder, Personal communication NIST, Oct. 1999.
[13] J. Crank, The Mathematics of Diffusion, 2nd ed., University Press, Oxford, 1975, 414 pp.
[14] T.C. Powers, The air requirement of frost resistant concrete, Highw. Res. Board Proc. 29 (1949) 184–211 (Washington. DC).
[15] K. Snyder, A numerical test of air void spacing equations, Adv. Cem. Based Mater. 8 (1998) 28–44.
[16] K. Snyder, J.R. Clifton, L.I. Knab, Freeze/thaw susceptibility of HPC, Wiss. Z. Hochsch. Archit. Bauwes, Weimar 40 (1994) 139–142.
[17] L.-O. Nilsson, Hygroscopic Moisture in Concrete—Drying, Measurements and Related Material Properties, Report TVBM-1003, Lund, Sweden, 1980, 162 pp.
[18] D. Bager, S. Jacobsen, A model for the destructive mechanism in concrete caused by freeze/thaw action, in: D.J. Janssen, M.J. Setzer, M.B. Snyder (Eds.), RILEM Proceedings PRO 25, Cachan, France, 2002, pp. 17–40.
[19] D. Bager, S. Jacobsen, A conceptual model for the freeze/thaw damage of concrete, in: K. Fridh (Ed.), Proc. 3rd Nordic Res. Seminar, Report TVBM-3056, Lund, Sweden, 1999, pp. 1–19.
[20] T.C. Powers, A working hypothesis for further studies of frost resistance of concrete (with discussion by R. Terzagi et al.), J. ACI 16 (4) (1945) 245–272.
[21] L.-O. Nilsson, Presentation at Workshop following Int. Conf on Ion and Mass transport in Concrete, Univ. of Toronto, Canada, October 6, 1999.
[22] G. Hedenblad, Moisture Permeability of Mature Concrete, Cement Mortar and Cement Paste, Report TVBM-1014, Lund, Sweden, 1993, 250 pp.
[23] S. Lindmark, Mechanisms of Salt Frost Scaling of Portland Cement-Bound Materials: Studies and Hypothesis, Report TVBM 1017, Lund, Sweden, 1998, 266 pp.
[24] J. Kaufmann, Experimental identification of damage mechanisms in cementitious porous materials on phase transition of pore solution under frost deicing salt attack, EPFL/EMPA These No. 2037, Switzerland, 1999, 193 pp.
[25] L. Tang, D. Bager, S. Jacobsen, H. Kukko, Evaluation of the ultrasonic method for detecting freeze/thaw cracking in concrete, SP Report 1997:37, Nordtest-project No. 1321-97, Borås, Sweden, 1997, 63 pp.
[26] S. Jacobsen, D. Bager, H. Kukko, L. Tang, K. Nordström, (1999) Measurement of internal cracking as dilation in the SS 137244 test, Norw. Build. Res. Inst. Project Report 250, Nordtest project 1389-98, Oslo, 26 p. + 5 app.
[27] K. Snyder, Personal communication NIST, May 2000.
[28] L. Tang., D. Bager, S. Jacobsen, H. Kukko, G. Gudmundsson, Evaluation of the modified slab test for resistance of concrete to internal frost damage, SP Report 2000:34, Nordtest-project No. 1485-00, Borås, Sweden, 2001.
[29] B. Zuber, J. Marchand, Modeling the deterioration of hydrated cement systems exposed to frost action: Part 1. Description of the mathematical model, Cem. Concr. Res. 30 (2000) 1929–1939.
[30] G. Fagerlund, K. Nordström, Studies of the internal frost resistance of HPC, Proc. 5th Int symp HPC, Norw Conc Ass., Oslo, Norway, 1999, pp. 1092–1103.
[31] M.T. Jepsen, Salt frost scaling-interaction of transport mechanisms and ice formation in concrete, in: M.J. Setzer, R. Auberg, H.J. Keck (Eds.), RILEM Proc. PRO, vol. 24, 2002, pp. 179–186.